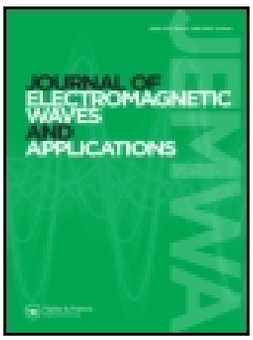

Journal of Electromagnetic Waves and Applications

ISSN: 0920-5071 (Print) 1569-3937 (Online) Journal homepage: https://www.tandfonline.com/loi/tewa20

Impacts of continuous modes approach on the back-off efficiency of Doherty power amplifiers

Gideon Naah, Songbai He, Weimin Shi, Caoyu Li & Rocco Giofrè

To cite this article: Gideon Naah, Songbai He, Weimin Shi, Caoyu Li & Rocco Giofrè (2019): Impacts of continuous modes approach on the back-off efficiency of Doherty power amplifiers, Journal of Electromagnetic Waves and Applications

To link to this article: https://doi.org/10.1080/09205071.2019.1607566

Published online: 19 Apr 2019.

JOURNAL OF ELECTROMAGNETIC WAVES AND APPLICATIONS
https://doi.org/10.1080/09205071.2019.1607566

Taylor & Francis
Taylor & Francis Group

Impacts of continuous modes approach on the back-off efficiency of Doherty power amplifiers

Gideon Naah [a], Songbai He[a], Weimin Shi[a], Caoyu Li[a] and Rocco Giofrè[b]

[a]School of Electronic Science and Engineering, University of Electronic Science and Technology of China, Chengdu, People's Republic of China; [b]Electronic Engineering Department, University of Roma Tor Vergata, Roma, Italy

ABSTRACT

This paper analyses the impacts of the harmonic-tuned hybrid continuous modes (HTHCMs) approach on the back-off efficiency of Doherty power amplifiers (DPAs). Based on the HTHCMs strategy, formulations are derived for designing the impedance inverting network (IIN) and impedance transforming network (ITN) in the DPA. Via the proposed approach, multiple impedance solutions for realizing broadband DPAs with substantial output back-off efficiency recovery is made possible. The potentiality of the design method is demonstrated by the realized prototype working from 1.4 to 2.45 GHz. Test results have shown over 50% drain efficiency at 6 dB back-off power.

ARTICLE HISTORY
Received 20 November 2018
Accepted 8 April 2019

KEYWORDS
Broadband Doherty PA; back-off efficiency; harmonic-tuned hybrid continuous modes; impedance inverting network; impedance transforming network

1. Introduction

To cope with the continuous request of a higher and higher data rate, wireless communication systems exploit signals with high peak-to-average power ratio (PAPR), posing severe challenges for power amplifiers (PAs). Among them, broadband operation, high back-off efficiency and spectral purity are the primary ones.

Considering the research effort of last years, the Doherty approach is probably the most suitable power amplifier (PA) architecture to meet such challenges [1–3].

Several techniques for adequately meeting the broadband and high back-off efficiency requirements in the Doherty power amplifier (DPA) are reported in the literature. Among these techniques are the bias modulation, envelope tracking [1], continuous mode [2] and many others [3–8]. Although the DPA's performance in [2] is encouraging, continuous mode analysis was not provided. Rather, the design is based on the de-embedded device model of the active devices. Also, it has limited bandwidth and larger circuit size.

In this article, harmonic-tuned hybrid continuous modes (HTHCMs) are proposed and applied to recover and further improve the DPA's back-off efficiency and bandwidth. The term "recover" in this context, is to redefine, reanalyze, retrieve and further enhance the efficiency lost at back-off using derived equations based on the HTHCMs in analysis. The

CONTACT Gideon Naah engrgnaah7@gmail.com School of Electronic Science and Engineering, University of Electronic Science and Technology of China, Chengdu 611731, People's Republic of China

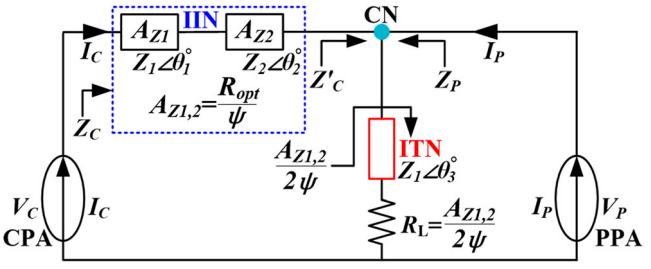

Figure 1. Simplified DPA schematic with the impedance inverting network (IIN) and impedance transforming network (ITN) for analysis.

validity and efficacy of the proposed approach is proved via the realized DPA prototype with 54.55% bandwidth and over 50% drain efficiency at 6 dB back-off power.

2. Theory of the proposed approach

Considering the simplified DPA schematic shown in Figure 1, V_c and I_c indicate the voltage and current of the carrier PA (CPA) whereas V_p and I_p indicate the voltage and current of the peaking PA (PPA), respectively, Z_c designates the impedance seen by the CPA at the power back-off level while Z'_c denotes the impedance seen by the CPA at the saturation power level, Z_p represent the impedance seen by the PPA at the saturation power level and R_L defines the impedance seen by both amplifiers at the load. The impedance inverting network (IIN) shown in Figure 1 causes the resistive impedance seen by the CPA to reduce as the PPA current I_p increases. The impedance transforming network (ITN) also shown in Figure 1 transforms the standard 50 Ω load to the optimum continuous mode load impedance (R_{opt}) at the combining node (CN). Derivations for the HTHCMs to be used in the analysis and design of the DPA are with the assumptions that the DPA's current waveforms meet the condition of the standard Class-B mode shown below for convenience [9]:

$$i_d(\theta) = I_{peak}\left(\frac{1}{\pi} + \frac{1}{2}\cos(\theta) + \frac{2}{3\pi}\cos(2\theta)\right) \tag{1}$$

where I_{peak} is the peak current amplitude. The voltage waveform of the HTHCMs for convenience is also stated as [10]:

$$v_d(\theta) = V_{DD}(1 - \alpha\cos(\theta) + \beta\cos(3\theta))(1 - \gamma\sin(\theta)) - 1 \le \gamma \le 1 \tag{2}$$

where V_{DD} is the drain bias voltage, α is the varying parameter for the continuous mode condition having a rigorous relationship with β and for keeping the voltage from crossing zero. ψ introduced in Figure 1 is the HTHCMs operation parameter needed for: reducing the transformation ratio in the IIN and ITN without bandwidth and efficiency limitations, suitable matching, and producing IIN and ITN that are not dependent on the center frequency to operate. In the case of the classical DPA, the IIN and ITN are designed at the center frequency to operate. When the IIN and ITN deviate from the center frequency, it incurs performance deteriorations in the DPA. With ψ, a rigorous relationship based on the HTHCMs can be redefined and reanalyzed between the IIN and ITN at back-off and saturation. Moreover, ψ compensates the effect of the impedances in the CPA and PPA. Also,

multiple impedance solutions space for realizing broadband DPAs with substantial back-off efficiency recovered may be possible. Proper output loading conditions cannot be precisely attained due to the known matching limitations in the DPA. Therefore, from Figure 1, the CPA's impedance transformation ratio is expressed as:

$$Z_C = \frac{A_{z1,2}^2}{Z_C'}, Z_C' = R_L\left(1 + \frac{I_P A_{z1,2}}{V_C}\right) \tag{3}$$

where $A_{z1,2}$ are the characteristic impedances of the quarter-wave lines in the IIN. In [9], $I_C = (I_{peak}/4)(1+\xi)$ and $I_P = (I_{peak}/2)(\xi)$. Therefore considering Ohm's law ($V_C = I_C Z_C$), (3), and the I_C and I_P equations in [9], the output voltage of the CPA becomes:

$$V_C = \frac{\left(\frac{I_{peak}}{4}\right)(1+\xi)A_{z1,2}^2}{R_L\left(1 + \left(\frac{I_{peak}}{2}\right)\xi\left(\frac{A_{z1,2}}{V_C}\right)\right)} \tag{4}$$

where ξ is 0 at 6 dB back-off power and 1 at the maximum power. After some rearrangement, (4) becomes:

$$V_C = A_{z1,2}\left(\frac{I_{peak}}{2}\right)\left(\frac{A_{z1,2}}{2R_L} + \xi\left(\frac{A_{z1,2}}{2R_L}\right)\right). \tag{5}$$

Then, the output voltage remains constant at V_{dc} while V_C is independent of ξ. For expediency in the HTHCMs analysis,

$$\frac{A_{z1,2}}{2R_L} = \psi, R_L = \frac{A_{z1,2}}{2\psi} \tag{6}$$

From $R_{opt} = (2V_{dc}/I_{peak})$ for the Class-B mode in [9], $(A_{z1,2}/2R_L) = (2V_c/I_{peak})$ with $V_C = V_{dc}$ in (5), and from (6),

$$A_{z1,2} = \frac{R_{opt}}{\psi} \tag{7}$$

Based on (6) and (7), ψ finally becomes:

$$\psi = \sqrt{\frac{R_{opt}}{2R_L}} \tag{8}$$

Note, $A_{z1,2}$ parameter remains at R_{opt} in (7) and (8) with the intention of increasing device reliability in the usage of the HTHCMs technique. Thus, on the condition that an inappropriate impedance match occurs, the alternative impedance match for the HTHCMs technique to fall on will be the $A_{z1,2}$ parameter. However, it is normalized to unity for convenience in analysis. The impedance of the PPA at saturation (Sat) and back-off (BO), respectively, denoted by Z_P and Z_P' are as follows:

$$Z_P = R_L\left(1 + \frac{I_C}{I_P}\right)@Sat, \qquad Z_P' = \infty\,@\,BO \tag{9}$$

To determine the fundamental and second harmonic impedances of the HTHCMs, i.e. Z_1 and Z_2, respectively, Z_C, Z_C' and Z_P are taken into consideration. This is done to examine

how $Z_1$and Z_2 impact the IIN and ITN. Therefore, from (1), (2), (3), (8) and (9), $Z_1$and Z_2 may be derived as:

$$Z_1 = R_{opt} \cdot Z_n \left(\left(\sqrt{2} \left(\frac{2}{3\sqrt{3}} \right) + \alpha \sin(\beta \cdot \gamma)\psi \right) + j * \left(\sqrt{2} \left(\frac{20}{3\sqrt{3}} \right) + \beta \cos(\alpha \cdot \gamma)\psi \right) \right)$$

$$Z_2 = R_{opt} \cdot Z_n \left((\sin(\psi + \beta)\alpha) - j * \left(\frac{3\pi}{8} \cos(\psi - \beta - \alpha)\gamma \right) \right)$$

$$Z_3 = \infty \tag{10}$$

where $Z_n = Z_C \cdot Z_C' \cdot Z_P$, α and ψ have a rigorous relationship with β in determining the HTHCMs operation. Thus, to keep v_d positive and the efficiency above the standard Class-B. With (10), the suitable characteristic impedances of the HTHCMs required by the IIN and ITN in ensuring the DPA's back-off efficiency and bandwidth are recovered and enhanced, are activated.

To further examine the inner working dimensions of the IIN and ITN at 6 dB back-off, the subsequent respective mathematical derivations are necessary and it is assumed they have fixed electrical lengths of 90°:

$$Z_{IIN} = \beta_i \sqrt{2Z_1 Z_2 \psi}\theta_{1,2}, \beta_i = 0.501@_{6dB-BO} \tag{11}$$

$$Z_{ITN} = \beta_i \sqrt{2Z_1 \psi}\theta_3, \beta_i = 0.501@_{6dB-BO} \tag{12}$$

where $\theta_{1,2,3}$ is the phase required between the IIN and ITN and can be written as $\theta_{1,2,3} = \pi/2 \cdot f_d$ (f_d is the desired frequency of the DPA, Z_{IIN} and Z_{ITN} are the impedances seen at their inputs, and $\beta_i = 10^{(OBO/20)}$ is the back-off ratio with $OBO = -20\log(x)$ in [dB] and $x = 2$ for 6dB-BO). Via (11) and (12), the IIN and ITN will be characterized and to aid (10) in recovering and improving the back-off efficiency of the DPA and its bandwidth extension.

Suppose that a parameter is introduced to examine the DPA's performance at back-off designated by ρ, it may be expressed as:

$$\rho = \left(\frac{\frac{1}{6\sqrt{3}} - (BO + \psi_\eta)}{\frac{1}{6\sqrt{3}} - 2 + 4(BO \cdot (\psi_\eta))} \right) \tag{13}$$

where BO (i.e. 0.501) specifies the 6 dB back-off operation of the DPA and ψ_η is the additional efficiency emanating from the HTHCMs. From (1), (2) and (13), the fundamental output power (P_{out}) and back-off efficiency (η_{BO}) can be, respectively, derived as:

$$P_{out} = \frac{V_{DD} \cdot I_{peak}}{4\rho} \tag{14}$$

$$\eta_{BO} = \frac{\pi}{4\rho} \tag{15}$$

Via the combination of (10) and (15), multiple impedance solutions space for over 50% η_{BO} is evidently depicted in Figure 2.

For the multiple impedance solutions space provided by the HTHCMs for the IIN and ITN in the DPA design, the load impedances taken by ψ are at $\psi = 9/10$, $\psi = 19/20$ and $\psi = 6/3\sqrt{3}$. Hence, the proposed HTHCMs provides bandwidth extension with the η_{BO} exhibiting ψ_η times higher efficiency recovery and enhancements at 6 dB back-off.

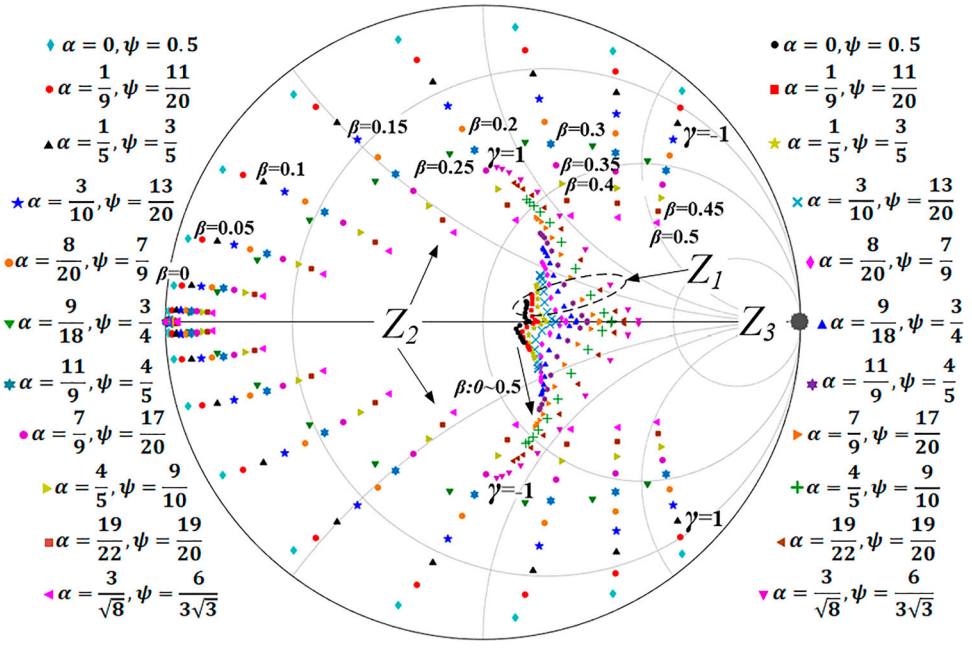

Figure 2. Multiple harmonic impedance solutions space for $\eta_{BO} > 50\%$ when $\psi = 9/10$, $\psi = 19/20$ and $\psi = 6/3\sqrt{3}$.

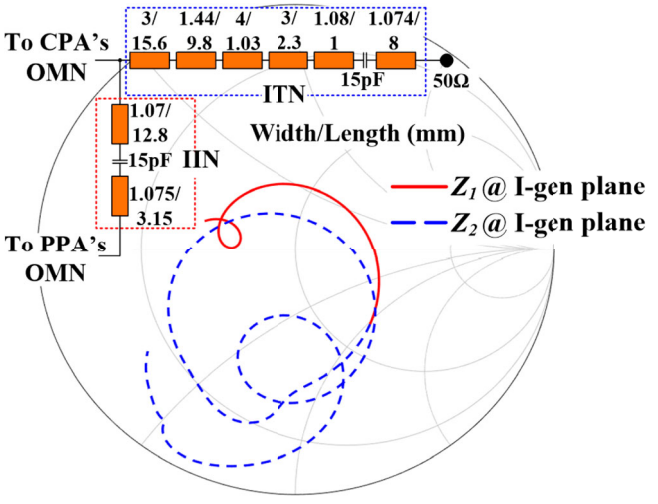

Figure 3. Synthesized DPA's IIN and ITN and their corresponding impedance trajectories at the I-gen plane with R_{opt} denormalised and set at 36 Ω in Smith chart.

2.1. Design of broadband DPA based on the HTHCMs

By performing load-pull simulations, the initial load impedances of the carrier and peaking amplifiers are obtained at the current-generator (I-gen) plane. Intensive computations are then carried out via (8) in order to find the optimal load impedances for

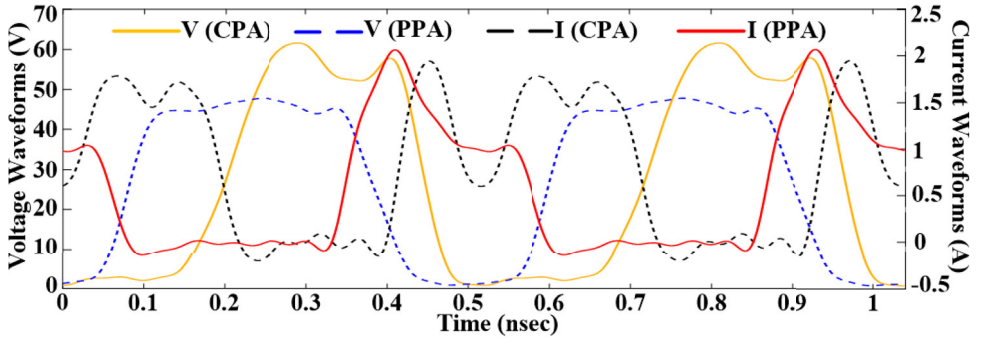

Figure 4. Simulated HTHCMs current and voltage waveforms of the DPA.

the carrier and peaking amplifiers required at the back-off and saturation power levels when the DPA is in operation. According to the acquired load impedances from the load-pull simulations, the initial load impedance obtained for the CPA is 15.31 + j*5.24 Ω while that of the PPA is 11.09-j*15.85 Ω. Then, the next step is to add the real parts of the impedances obtained for both the CPA and PPA which is 15.31 + 11.09 Ω. In other words, the real part of the obtained impedance pertaining to the CPA is 15.31 Ω while that of the PPA is 11.09 Ω. Consequently, an impedance of 26.4 Ω is acquired. The real parts of the obtained impedances give more design freedom for realizing broadband high efficiency HTHCMs-DPAs. Then, using (8), substitute R_{opt} with 26.4 Ω. About 0.5 is obtained for ψ. After this, sweep ψ from 0.5 to $2R_L$ for efficient analysis at the back-off and saturation power levels. In other words, sweeping ψ from 0.5 to $2R_L$ provides a greater possibility of acquiring a suitable matching in the DPA. Otherwise, the performance of the DPA will be degraded due to not having a more extensive design space. In this manner, causing difficulty in an optimal impedance match. The extensiveness acquired through the continuum mode active load modulation as shown in Figure 2, guarantees the more extensive design space for substantial performance enhancements. Based on the continuum mode active load modulation, R_{opt} is matched to $2R_L$ by the IIN. The main idea behind sweeping ψ is that in the literature the performance of continuous mode PAs are usually worse than the theoretical results. This is due to the inability of the network not finding a suitable matching. In view of this limitation, the proposed method might be more suitable and practical in finding the appropriate impedance solutions design space where optimal matching is guaranteed. Consequently, the optimal impedance of the carrier amplifier required at back-off (Z_C) is 10 Ω while that at saturation (Z'_C) is 20 Ω. In the case of the peaking amplifier, the optimal impedance required at saturation (Z_P) is 40 Ω. The impedances of (10)–(12) are carefully tuned to ensure substantial 6 dB η_{BO} recovery and bandwidth extension.

Furthermore, considering the working band of the proposed DPA, Z_1 and Z_2 are, respectively, set at 1.5 GHz (50 Ω) and 2.5 GHz (49.98 Ω) in the IIN whereas in the ITN, Z_1 is further tuned for maximum power transfer. Also, $\theta_1 = 38.6°$, $\theta_2 = 15.85°$ and $\theta_3 = 117°$ are the obtained electrical lengths. The ITN attached to the output matching network of the CPA aided in enhancing the gain, η_{BO} and bandwidth of the DPA. This approach differs from the classical one which uses the center frequency in designing the IIN and ITN as well as attaching the ITN to the output matching network of the PPA. The output matching

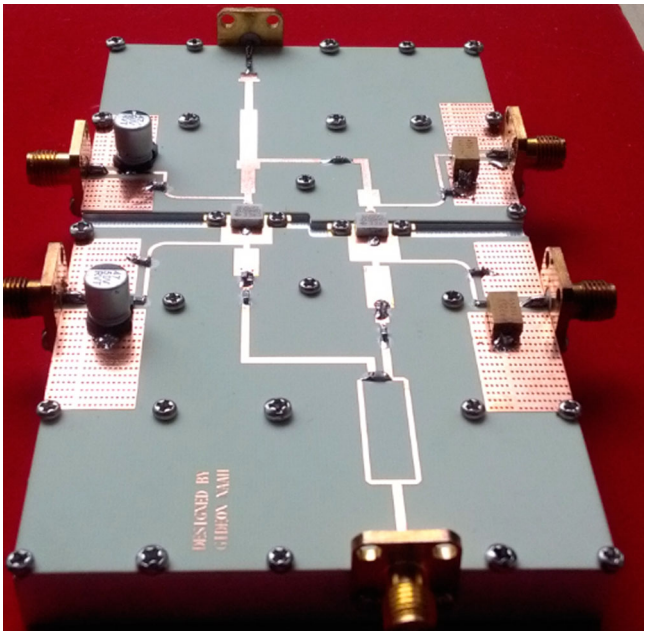

Figure 5. Photograph of the fabricated DPA prototype.

networks of the CPA and PPA are judiciously devised to ensure they do not degenerate the performance of the IIN and ITN at back-off. The synthesized IIN and ITN and their corresponding impedance trajectories at the I-gen plane are depicted in Figure 3. In this case, the impedances at the I-gen plane are denormalized with R_{opt} set at 36 Ω as a reference. This is done to ensure the HTHCMs condition operation. The current and voltage waveforms of the DPA from which the HTHCMs are evident are shown in Figure 4. As shown in Figure 3, Z_1 and Z_2 terminations are within the regions shown in Figure 2. Thus, they are in conformity with the analysis, supporting the feasibility of the proposed HTHCMs design strategy.

3. Simulation and experimental results

A DPA prototype is implemented using Wolfspeed's CGH40010F GaN HEMT. The DPA is fabricated on a Rogers RO4350B substrate with $h = 20$ mil and $\varepsilon_r = 3.66$. The working frequency band of the DPA ranges from 1.4 to 2.45 GHz, corresponding to 54.55% bandwidth. The gate bias of the CPA is set at −2.9 V while that of the PPA is set at −5.6 V. A drain bias of 28 V is used for both sub-amplifiers in measurement. Figure 5 shows the photograph of the fabricated DPA.

The simulated DPA results under continuous wave signals are shown in Figure 6. Figure 6(a) shows the simulated drain efficiency (DE) and gain as a function of output power (Pout), depicting the classic Doherty efficiency profiles while Figure 6(b) shows the simulated gain as a function of Pout. Depicted in Figure 6(c) is the simulated DE over operating frequency at saturation and 6dB-BO power levels. Likewise, Figure 6(d) shows the simulated Pout over operating frequency at saturation and 6dB-BO power levels. As shown in the

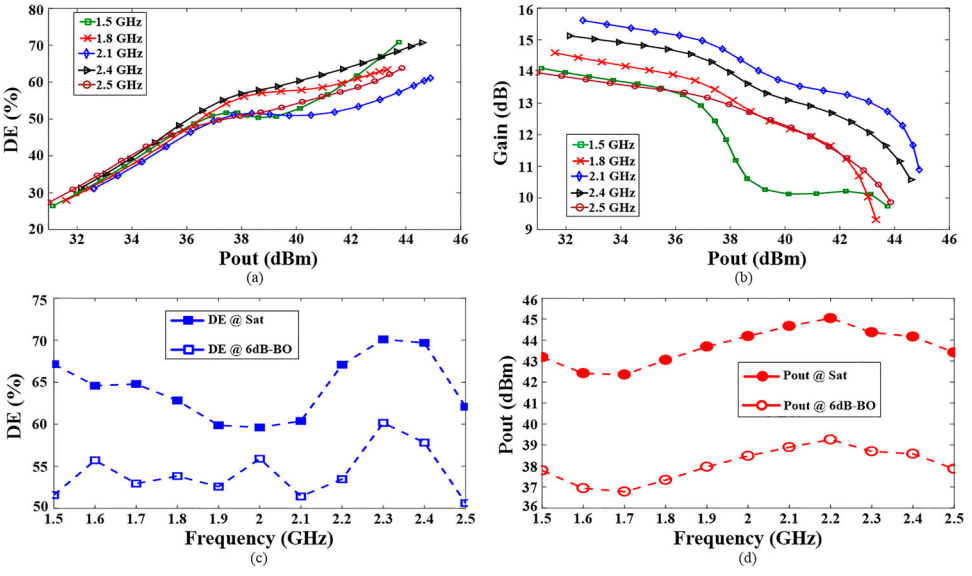

Figure 6. (a) Simulated drain efficiency (DE) as a function of output power (Pout). (b) Simulated gain as a function of Pout. (c) Simulated DE over operating frequency at Sat and 6dB-BO. (d) Simulated Pout over operating frequency at Sat and 6dB-BO.

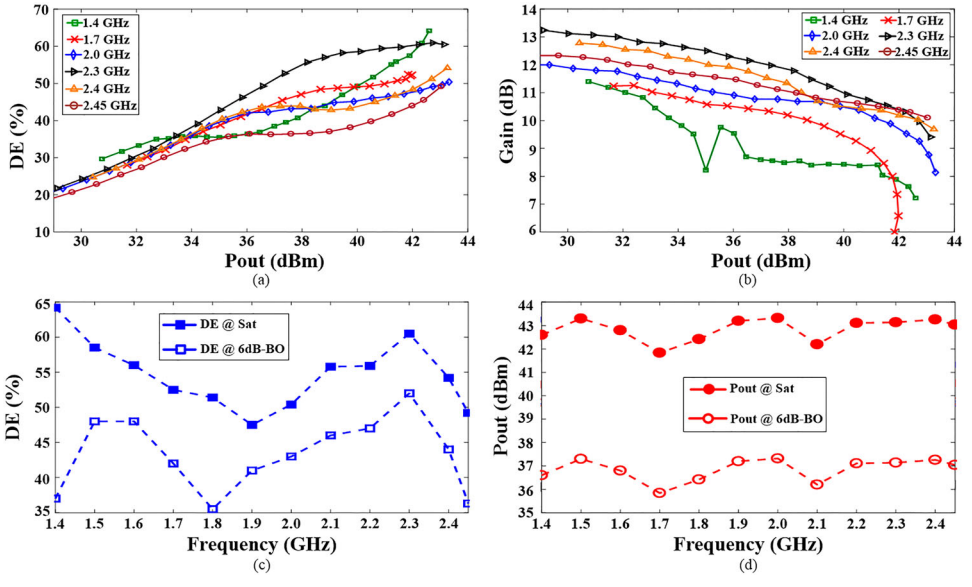

Figure 7. (a) Measured drain efficiency (DE) as a function of output power (Pout). (b) Measured gain as a function of Pout. (c) Measured DE over operating frequency at Sat and 6dB-BO. (d) Measured Pout over operating frequency at Sat and 6dB-BO.

Figures 6(c) and (d), at 6dB-BO power level, more than 58% DE and 38 dBm Pout are, respectively, obtained. The maximum DE (60.2%) and Pout (39.3 dBm) at 6dB-BO are recorded at 2.3 and 2.2 GHz, respectively. In the entire working frequency band, the recorded DE, Pout

Table 1. Comparison with some reported broadband DPAs

Ref.	Bandwidth (GHz) (%)	Pout (dBm)	Gain (dB)	DE@Sat (%)	DE@6dB-BO (%)
2017 [2]	1.7–2.7 (45.5)	52.7–54.3	12.3–13.7	53–66	40–50.2
2016 [3]	1.5–2.5 (50)	42–44.5	8–11	55–75	42–53
2017 [4]	1.5–2.4 (46)	43.1–44.4	–	57–74	45–56
2018 [5]	1.5–2.6 (53.6)	41.8	18.2–20.4	40–45	31–35
2014 [6]	1.05–2.55 (83)	40–42	7–9	45–83	35–58
2017 [7]	0.55–1.1 (67)	42–43.5	$> 10^*$	56–72	40–52
2019 [8]	1.1–2.4 (74)	43.5–45.4	9.5–11.1	55.4–68	43.8–54.9
This work	1.4–2.45 (54.55)	41.84–43.52	6–13	47.5–64.2	35.5–52

DE: drain efficiency, *: estimated from the figure.

and gain ranges from 58.7% to 71.1%, 42.3 dBm–45.3 dBm and 9.3 dB–12.3 dB, respectively, at saturation power level.

The measured results of the DPA under continuous wave excitation are shown in Figure 7. Figure 7(a) shows the measured DE as a function of Pout, approximately depicting the classic Doherty efficiency profiles. Figure 7(b) shows the measured gain as a function of Pout while Figure 7(c) presents the measured DE over operating frequency at saturation and 6dB-BO power levels. Finally, Figure 7(d) shows the measured Pout over operating frequency at saturation and 6dB-BO power levels. In Figure 7(c), it is very obvious the DPA recorded more than 58.7% DE at saturation power level. At 6 dB BO power level, more than 50% DE is successfully achieved. The performance of the DPA extended well below the design band.

This work is compared with some reported DPAs in Table 1. From Table 1, it is apparent that the performance of our DPA shows comparable results.

4. Conclusion

The impacts of harmonic-tuned hybrid continuous modes (HTHCMs) approach on the back-off efficiency of Doherty power amplifiers have been presented in this work. For verification, a broadband Doherty power amplifier prototype was implemented working from 1.4 to 2.45 GHz, accounting for 54.55% bandwidth. Test results have shown over 50% drain efficiency at 6 dB back-off power.

Disclosure statement

No potential conflict of interest was reported by the authors.

Notes on contributor

Dr. Rocco Giofrè was born in Vibo Valentia, Italy, in 1979. He received the M.S.Eng. degree (summa cum laude) in electronic engineering and the Ph.D. degree in space systems and technologies from the University of Roma Tor Vergata in 2004 and 2008, respectively. He is currently a Tenure Tack Assistant Professor with the Electronics Engineering Department, University of Roma Tor Vergata. He has authored or coauthored over 160 scientific papers. His research interests include RF power amplifier theory, design and test, linearization techniques, and efficiency improving techniques. He was a recipient of the 2005 Young Graduated Research Fellowship presented by the Gallium Arsenide application Symposium Association and the Best Paper Award at the 2nd EuMIC Conference in 2007.

ORCID

Gideon Naah http://orcid.org/0000-0002-2409-1942

References

[1] Camarchia V, Pirola M, Quaglia R, et al. The Doherty power amplifier: review of recent solutions and trends. IEEE Trans Microw Theory Techn. Feb. 2015;63(2):559–571.
[2] Chen X, Chen W, Zhang Q, et al. A 200 watt broadband continuous-mode Doherty power amplifier for base-station applications. IEEE MTT-S Int Microw Symp Dig. June 2017: 1110–1113.
[3] Chen S, Wang G, Cheng Z, et al. A bandwidth enhanced Doherty power amplifier with a compact output combiner. IEEE Microw Wireless Compon Lett. Jun. 2016;26(6):434–436.
[4] Chen P, Xia J, Merrick BM, et al. Multiobjective Bayesian optimization for active load modulation in a broadband 20-W GaN Doherty power amplifier design. IEEE Trans Microw Theory Techn. March 2017;65(3):860–871.
[5] Khan MS, Zhang H, Wang X, et al. A novel two-stage broadband Doherty power amplifier for wireless applications. IEEE Microw Wireless Compon Lett. Jan. 2018;28(1):40–42.
[6] Giofr'e R, Piazzon L, Colantonio P, et al. A closed-form design technique for ultra-wideband Doherty power amplifiers. IEEE Trans Microw Theory Techn. Dec. 2014;62(12):3414–3424.
[7] Darraji R, Bhaskar D, Sharma T, et al. Generalized theory and design methodology of wide-band Doherty amplifiers applied to the realization of an octavebandwidth prototype. IEEE Trans Microw Theory Techn. Aug. 2017;65(8):3014–3023.
[8] Yang Z, Yao Y, Li M, et al. Bandwidth extension of Doherty power amplifier using complex combining load with noninfinity peaking impedance. IEEE Trans Microw Theory Techn. Feb. 2019;67(2):765–777.
[9] Cripps SC. RF power amplifiers for wireless Communications. 2nd ed Norwood (MA): Artech House; 2006.
[10] Chen J, He S. Broadband high-efficiency power amplifiers design based on hybrid continuous modes utilizing the optimal impedances at package plane. IEEE MTT-S Int Dig. May 1722;2015:14.